# NJC

Accepted Manuscript

This is an *Accepted Manuscript*, which has been through the Royal Society of Chemistry peer review process and has been accepted for publication.

Accepted Manuscripts are published online shortly after acceptance, before technical editing, formatting and proof reading. Using this free service, authors can make their results available to the community, in citable form, before we publish the edited article. We will replace this *Accepted Manuscript* with the edited and formatted *Advance Article* as soon as it is available.

You can find more information about *Accepted Manuscripts* in the **Information for Authors**.

Please note that technical editing may introduce minor changes to the text and/or graphics, which may alter content. The journal's standard **Terms & Conditions** and the **Ethical guidelines** still apply. In no event shall the Royal Society of Chemistry be held responsible for any errors or omissions in this *Accepted Manuscript* or any consequences arising from the use of any information it contains.
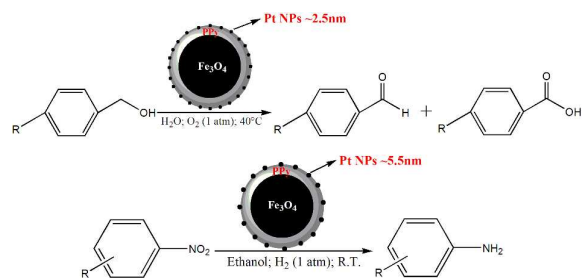
www.rsc.org/njc

Size effects of supported Pt nanoparticles were entirely different for benzylic alcohols aerobic oxidation and hydrogenation reduction of nitroaromatics

ARTICLE TYPE

Distinctive size effects of Pt nanoparticles immobilized on Fe$_3$O$_4$@PPy used as an efficient recyclable catalyst for benzylic alcohols aerobic oxidation and hydrogenation reduction of nitroaromatics

Yu Long, Bing Yuan, Jianrui Niu, Xin Tong, Jiantai Ma*

Fe$_3$O$_4$@PPy composite microspheres have been synthesized using Fe$_3$O$_4$ microspheres as a chemical template under an ultrasonic treatment process. Pt nanoparticles (NPs) were immobilized onto Fe$_3$O$_4$@PPy by using ethylene glycol (EG) and NaBH$_4$ as reducing agent. The information of the
10 morphologies, sizes, and dispersion of Pt NPs of the as-prepared catalysts was verified by TEM, XRD, FTIR and XPS. As expected, the chemical reduction methods remarkably affected the size of Pt NPs (~2.5nm and ~5.5nm, respectively) and the prepared catalysts exhibited high catalytic activities as well as awsome stabilities for aerobic oxidation of benzylic alcohols and hydrogenation reduction of nitroaromatics. It was highlighted that size effects for the catalytic properties of the two reactions were
15 found to be quite different. Fe$_3$O$_4$@PPy-Pt (2.5nm) afforded a higher conversion for benzylic alcohols aerobic oxidation, while the selectivities toward benzaldehyde over these two catalysts were similar. However, they showed almost same catalytic performance for hydrogenation reduction of a majority of nitroaromatics. What's more, Fe$_3$O$_4$@PPy-Pt (5.5nm) gave better activities of several nitroaromatics which were relatively difficult to be hydrotreated under the same conditions. In addition, the EG reduced
20 Fe$_3$O$_4$@PPy-Pt catalyst exhibited slightly poorer stability than the NaBH$_4$ reduced Fe$_3$O$_4$@PPy-Pt catalyst in the recycle tests, which might due to the agglomeration of small Pt NPs.

Introduction

The function of a heterogeneous catalyst with supported active component is determined by the complicated interplay of many
25 factors. The size of the active component is one of the most important factors in controlling the catalytic performance in many systems[1]. Nanosized particles of noble metals as active components have attracted much interest in recent years because of their size-dependent catalytic properties[2]. Among noble
30 metals, Pt NPs, with good resistance to corrosion and chemical attack[3], play a major role in many applications such as electrocatalysis[4], photocatalysis[5], biosensors[6] and other heterogeneous catalysis[7]. It is expected that, the size of Pt NPs may affect the electronic structure and the coordination structure
35 of the active site, and thus may influence the activation of reactant molecules and the active species, leading to differences in activity and/or selectivity[8]. Therefore, the deep understanding of the size effect of supported Pt NPs in various kinds of reactions would be very helpful for the rational design of highly
40 efficient catalysts.
However, Pt is not common and cheap enough for widespread application. So it is a big challenge to improve the efficiency, save resource and increase recycle rate. In recent years, there has been an increasing trend toward the use of magnetically
45 retrievable materials in a variety of areas[9]. Fe$_3$O$_4$ as a superior magnetic material, has been used in efficient green chemical

synthesis and biomedical sciences[10]. Moreover, interest in preparation of shell coated magnetic Fe$_3$O$_4$ microparticles is increasing dramatically. So far, different kinds of shell have been
50 reported to coat magnetic Fe$_3$O$_4$ microparticles[11]. Our team also has reported many works about synthesis and application of core-shell Fe$_3$O$_4$ supported nanoparticle catalysts[7b, 12]. The catalyst with magnetic particle core allows it to be facilely recovered and reused using an external magnet. And the shell coating Fe$_3$O$_4$
55 could forcefully fasten metal NPs by strong coordination effect, thus, avoiding metal NPs splitting from the support during the catalytic reaction.
In previous report, reduction method or reducing agent of platinum mainly include photodeposition, radiation-induced,
60 ethylene glycol, ethanol, sodium borohydride, hydrogen, sodium phosphinate, argon plasma and so on[13]. And size effects of supported Pt NPs have been used in nanoparticles-electrocalytic oxidation reaction. In this work, Fe$_3$O$_4$@PPy composite immobilize different sizes of Pt NPs using ethylene glycol and
65 sodium borohydride as classical reducing agent. And the information of the morphologies, sizes, and dispersion of Pt NPs for the as-prepared catalysts is investigated. Meanwhile, the size effects of Pt NPs are tested in aerobic oxidation of benzylic alcohols and hydrogenation reduction of nitroaromatics. It is
70 conceivable that catalytic activities of the two completely opposite reactions would give a relevant conclusion about sizes

effects of the supported Pt NPs catalysts. To our best knowledge, size effects of Pt NPs supported on magnetic core-shell material for different kinds of reaction have not been reported.

Experimental

Materials

Iron (III) chloride hydrate, sodium acetate, Poly-N-vinylpyrrolle-2-one (PVP, K-30), ethylene glycol, pyrrole, potassium chloroplatinite, hexachloroplatinic acid, ethanol were purchased from Sinopharm Chemical Reagent Co., Ltd. Various reaction reagents, such as 4-mthylbenzyl alcohol, 4-chlorobenzyl alcohol, 4-methoxybenzyl alcohol, 4-nitrobenzyl alcohol, 4-bromonitrobenzene, 4-nitroanisole, 4-methylnitrobenzene, 2, 5-dichloronitrobenzene, 1-nitronaphthalene and 4-chloromethylnitrobenzene, were purchased from Alfa Aesar. All chemicals were of analytical grade and used as received without further purification. Deionized water was used throughout the experiments

Preparations of Fe_3O_4@PPy-Pt catalysts

Fe_3O_4 microparticles were synthesized with the solvothermal method according to our previous Work[7b]. Firstly, 1.5 g $FeCl_3·6H_2O$, 1.0 g PVP and 2.0 g NaAc were added into 200 mL ethylene glycol. The mixture was stirred violently for 2 hours to make all materials dissolve completely. Then the mixture was transferred to a Teflon-lined stainless steel autoclave and sealed to heat at 200 °C for 8 h. The precipitated black product was collected from the solution by an external magnet and washed with deionized water and ethanol several times. Finally, the black product was dried in a vacuum for 24 h at 60°C.

Typically[12c], Fe_3O_4 microparticles (0.30 g) were dispersed in 70 mL H_2O under sonication, and then pyrrole (4 mL) in ethanol (15 mL) and HCl solution (15 mL, 6 M) were added into the above solution in turn under sonication for 1 h. Finally, the black product was collected with the help of a magnet, washed with deionized water and ethanol repeatedly to remove the residual pyrrole monomers and HCl acid, and then dried in a vacuum at 60°C for 12 h to get magnetic Fe_3O_4@PPy composite.

Syntheses of Fe_3O_4@PPy-Pt(EG). An aqueous solution of Fe_3O_4@PPy (100 mg) in deionized water (100 mL) was ultrasonicated for 1 h to form a uniform suspension. Subsequently, K_2PtCl_4-EG (0.005 M, 10 mL) solution was added to the suspension and sonicated for 2 h. The pH of the solution was adjusted to 10 using potassium hydroxide-EG (KOH-EG) solution (0.1 M), and then the solution was stirred under argon at 130°C for 3h. The precipitated black product was collected from the solution by an external magnet and washed with deionized water and ethanol. The step was repeated several times before drying in vacuum at 60°C for 24h.

Syntheses of Fe_3O_4@PPy-Pt($NaBH_4$). An aqueous solution of Fe_3O_4@PPy (100 mg) in deionized water (100 mL) was ultrasonicated for 1 h to form a uniform suspension. Then, an aqueous solution of H_2PtCl_6 (0.01 M, 5.6 mL) was added into the suspension under stirring and the mixture was stirred for 30 min at room temperature. Subsequently, the $NaBH_4$ solution (0.01 M, 50 mL) was delivered by drops into the above suspension under continuous stirring. After reacting for 3 h at room temperature, the precipitated black product was collected from the solution by an external magnet and washed with deionized water and ethanol several times and finally dried in a vacuum at 60°C for 12 h.

Characterizations of Fe_3O_4@PPy-Pt catalyst

These magnetic micro-materials were characterized inductively coupled plasma (ICP), powder X-ray diffraction (XRD), transmission electron microscopy (TEM), X-ray photoelectron spectroscopy (XPS), fourier transform-infrared (FT-IR) and vibrating sample magnetometry (VSM). XRD measurements were performed on a Rigaku D/max-2400diffractometer using Cu–Ka radiation as the X-ray source in the 2θ range of 5–80°. The size and morphology of the magnetic microparticles were observed by a Tecnai G2 F30 transmission electron microscopy and samples were obtained by placing a drop of a colloidal solution onto a copper grid and evaporating the solvent in air at room temperature. Pt content of the catalyst was measured by ICP on IRIS Advantage analyzer. Magnetic measurements of Fe_3O_4@PPy-Pt were investigated with a Quantum Design VSM at room temperature in an applied magnetic field sweeping from -8 to 8 kOe. XPS was recorded on a PHI-5702 instrument and the C1s line at 284.8 eV was used as the binding energy reference.

### Typical procedure for aerobic oxidation of benzylic alcohols

In a typical process, benzylic alcohols and Pt of Fe_3O_4@PPy-Pt with a mole ratio of 50 were dissolved in 5 mL deionized water. Then the reactions were carried out under oxygen atmosphere with electro-magnetic stirring at 40°C for a certain time. After the reaction, the aqueous phase was extracted five times with diethyl ether. Then the combined organic extracts were dried over $MgSO_4$ and analyzed by characterizing the reaction mixture using Gas Chromatograph-Mass Spectrometer (GC-MS).

Typical procedure for hydrogenation reduction of nitroaromatics

In a typical process, nitroaromatics and Pt of Fe_3O_4@PPy-Pt with a mole ratio of 200 were dissolved in 5 mL ethanol. Then the reactions were carried out under hydrogen atmosphere with electro-magnetic stirring conditions at room temperature for a certain time. The reaction was monitored and analyzed by characterizing the reaction mixture using GC-MS.

Results and Discussion

Preparation and characterizations of Fe_3O_4@PPy composite and Fe_3O_4@PPy-Pt catalyst
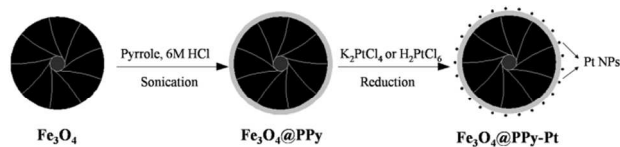
Scheme 1 Preparation process of catalysts

The process of preparation of the Fe_3O_4@PPy-Pt catalyst is schematically described in Scheme 1. Fe_3O_4 microparticles were synthesized with the solvothermal method according to our previous Work[7b]. Secondly, in the strong acidic solution, the Fe^{3+} released from Fe_3O_4 microspheres and the polymerization of pyrrole monomers occurred, thus a layer of polypyrrole was

coated on the surface of Fe_3O_4[12c]. Thirdly, under magnetic stirrers, K_2PtCl_4 and H_2PtCl_6 were reduced onto the surface of polypyrrole by EG and $NaBH_4$ to obtain Fe_3O_4@PPy-Pt catalysts.

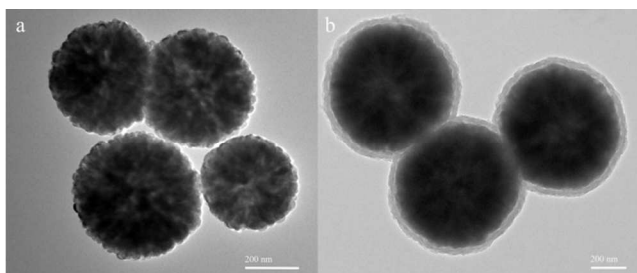5   Fig. 1 TEM images of (a) Fe_3O_4, (b) Fe_3O_4@PPy

Fig. 1a shows the typical TEM image of Fe_3O_4 microspheres prepared by the versatile solvothermal reaction. As can be seen from the image, the average diameter of the as-synthesized spherical particles was about 400 nm. The TEM image in Fig. 1b 10 showed that a continuous layer of PPy could be observed on the outer shell of the Fe_3O_4 microsphere cores and the thickness was about 35 nm. The resultant Fe_3O_4@PPy composites had good dispersibility and spherical morphology.

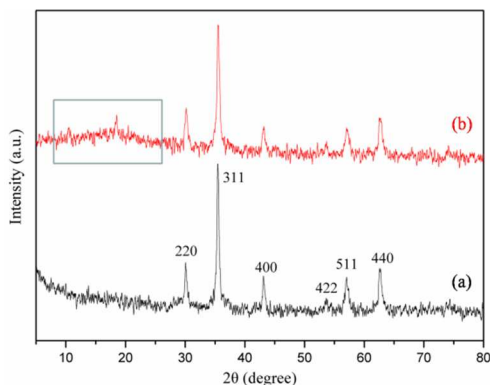15   Fig. 2 XRD patterns of (a) Fe_3O_4, (b) Fe_3O_4@PPy

The XRD pattern of Fe_3O_4 (Fig. 2a) and Fe_3O_4@PPy (Fig. 2b) showed characteristic peaks of magnetite microparticles and the sharp. The main peaks of the Fe_3O_4@PPy composite were similar to the Fe_3O_4, exhibiting that the coating process under acidic 20 conditions did not affect the structure of Fe_3O_4. Both of the two patterns showed strong peaks which confirmed the products were well-crystallized and detected diffraction peaks in every pattern could be indexed as cubic Fe_3O_4 (JCPDS card No. 82-1533). A broad peak was observed at $2\theta = 10° -25°$, which suggested 25 newly generating a layer of PPy[14].

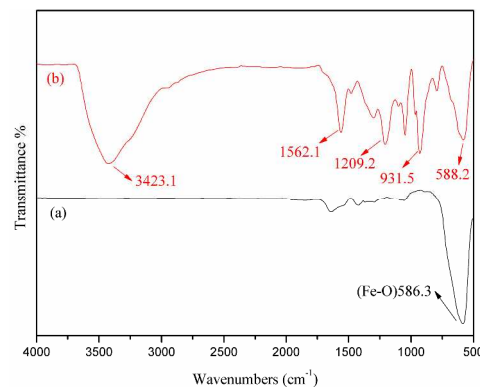Fig. 3 FT-IR patterns of (a) Fe_3O_4, (b) Fe_3O_4@PPy

The compositions of Fe_3O_4@PPy composite microsphere were confirmed by FT-IR (Fig. 3). As was also shown in the picture, in 30 the low-frequency region, the peak at 586.3 cm^{-1} (Fig. 3a), 582.5 cm^{-1} (Fig. 3b) corresponded to the stretching vibration peak of Fe-O. From the spectrogram, the peaks around at 1562 cm^{-1} (C=C stretching vibrations), 1209 cm^{-1} (C-N stretching vibrations), and 931 cm^{-1} (C-H stretching vibrations) revealed the presence of 35 PPy.
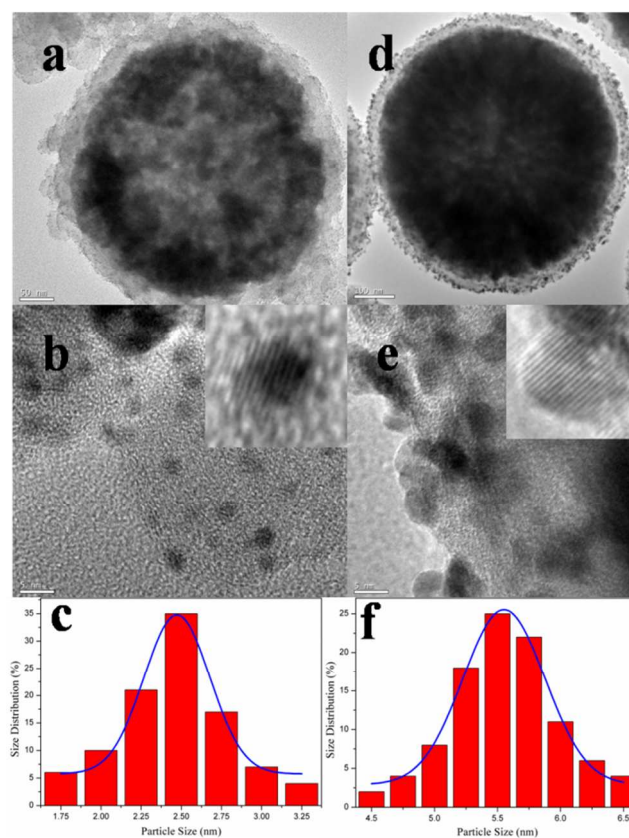

Fig. 4 TEM images of (a) Fe_3O_4@PPy-Pt(EG) and (d) Fe_3O_4@PPy-Pt($NaBH_4$); HRTEM images of (b) Fe_3O_4@PPy-Pt(EG) and (e) Fe_3O_4@PPy-Pt($NaBH_4$); particle size distribution of (c) Fe_3O_4@PPy-Pt(EG) and (f) Fe_3O_4@PPy-Pt($NaBH_4$)

40

The morphologies, the sizes, and the dispersion of Pt NPs deposited on Fe_3O_4@PPy had been investigated by TEM (Fig. 4). As exhibited in Fig. 4d, e and f, the Pt NPs reduced by $NaBH_4$ were randomly dispersed on Fe_3O_4@PPy with a wide size

distribution affording an average diameter of about 5.5 nm (Fig 4f). On the other hand, the Pt NPs got by using EG as reducing agent, which were observed with a narrow size distribution with a average diameter of about 2.5 nm (Fig 4c), were equably attached on the surface of Fe_3O_4@PPy (Fig. 4a, b). However, it possessed a more inferior crystal structure than that of the $Pt/NaBH_4$ (HRTEM in the inset image in Fig. 4b, e), which indicated $NaBH_4$ was a better reducing agent to forming perfect crystal structure of Pt NPs. Therefore, it was significant to control the reducing agents and reducing conditions for the design of the supported nanoparticle catalyst.
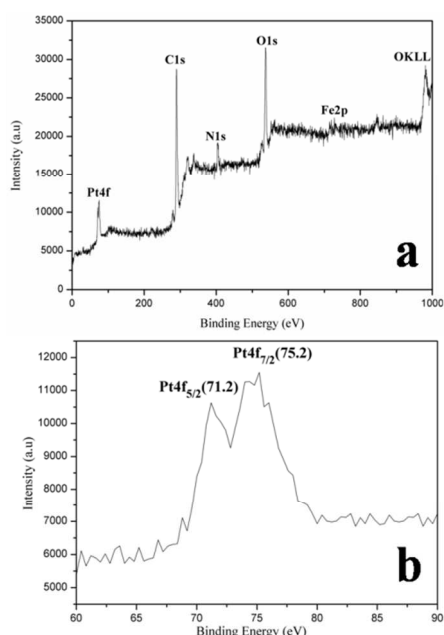

Fig. 5 XPS spectra for (a) Fe_3O_4@PPy-Pt(EG) and (b) Fe_3O_4@PPy-Pt(EG) showing Pd $3d_{5/2}$ and Pd $3d_{3/2}$ binding energies.

The XPS elemental survey scan of the surface of the Fe_3O_4@PPy-Pt(EG) was showed in Fig. 5a. Peaks corresponding to iron, oxygen, nitrogen, palladium and carbon were clearly observed. To ascertain the oxidation state of the Pt, XPS studies was carried out. The XPS analysis of the Pt (0) catalyst showed in Fig. 5b. As expected, the spectrum of the Pt 4f region confirmed the presence of Pt (0) with peak binding energy of 71.2 and 75.2 eV, which were assigned to Pt $4f_{5/2}$ and Pt $4f_{7/2}$, respectively.
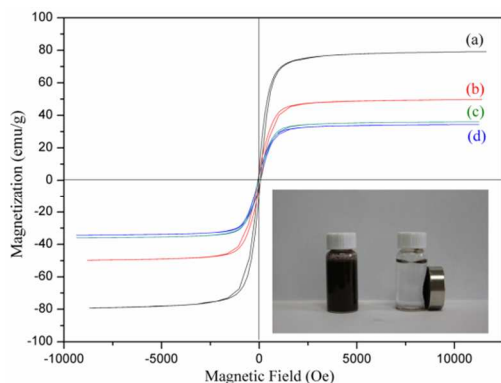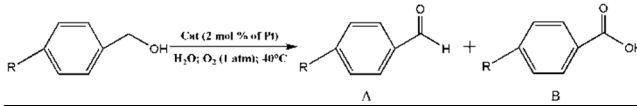

Fig. 6 VSM of (a) Fe_3O_4, (b) Fe_3O_4@PPy, (c) Fe_3O_4@PPy-Pt(EG) and (d) Fe_3O_4@PPy-Pt(NaBH_4)
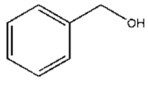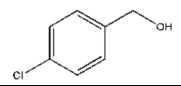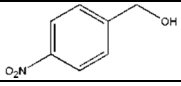
Since the ability of recoverability was important for this catalyst, magnetic measurements were performed using a VSM at room temperature. As shown in Fig. 6, Fe_3O_4@PPy (Fig. 6b), Fe_3O_4@PPy-Pt(EG) (Fig. 6c) and Fe_3O_4@PPy-Pt(NaBH_4) (Fig. 6d) showed small reduction of the saturation magnetization. This slightly reduction of the saturation magnetization for the material loaded solid was expected. The measured saturation magnetizations were 36.0 $emug^{-1}$ for Fe_3O_4@PPy-Pt(EG) (Fig. 6c) and 34.4 $emug^{-1}$ for Fe_3O_4@PPy-Pt(NaBH_4) (Fig. 6d). The decrease of the saturation magnetization suggested the presence of platinum nanoparticles on the surface of the magnetic support. Even with this reduction in the saturation magnetization, the catalyst could still be efficiently separated from solution with an external magnet as shown in the inset image in Fig. 6.
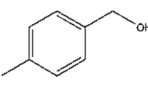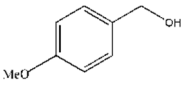
Catalyst testing for the aerobic oxidation of benzylic alcohols and hydrogenation reduction of nitroaromatics

For compare of the catalytic activity of the two Fe_3O_4@PPy-Pt catalysts, the benzylic alcohols aerobic oxidation and hydrogenation reduction of nitroaromatics were carried out under atmospheric pressure of O_2/H_2 as model reactions.

Table 1 Aerobic oxidation of various benzylic alcohols in water

Entry	Substrate	Catalyst	Time (h)	A Yield (%)	B Yield (%)
1		Pt/EG[a]	8	81	13
2		Pt/NaBH₄[b]	8	72	10
3		Pt/EG	8	75	12[c]
4		Pt/NaBH₄	8	70	10[d]
5		Pt/CNT-plasma	2	18[e]	
6		Pt/CNT-IMP	2	13[f]	
7		nPt@hC[g]	24	46	
8		Pt/AC[h]	24	44	
9		Pt/EG	6	93	4
10		Pt/NaBH₄	6	85	4
11		PS-PtNPs[i]	10	80	16
12		Pt/C[j]	10	60	10
13		K₂PtCl₄[k]	10	0	0
14		Pt/EG	6	96	<1
15		Pt/NaBH₄	6	87	<1
16		Pt/EG	10	82	15
17		Pt/NaBH₄	10	77	12
18		Pt/EG	12	74	9
19		Pt/NaBH₄	12	59	7

[a] Fe_3O_4@PPy-Pt(EG); [b] Fe_3O_4@PPy-Pt(NaBH₄); [c, d] Yield after 5 runs; [e,f] [ref 13f] conversion of benzyl alcohol. Reaction conditions: alcohol 1 mmol, deionized water 50 ml, catalyst 4mg (0.001 mmol Pt), O_2 flow rate 25 ml/min, T=75℃, t=2 h; [g, h] [ref 15a] Reaction conditions: catalyst 0.1 mol% of Pt, O_2 balloon, T=60 ℃, t=24 h; [i, j, k] [ref 15b] Reaction conditions: alcohol 0.5 mmol, deionized water 1 ml, catalyst 2.0 mol% of Pt, O_2 balloon, T=30 ℃, t=10 h;

Table 1 listed the catalytic performances of Fe_3O_4@PPy-Pt(EG) and Fe_3O_4@PPy-Pt(NaBH₄) in aerobic oxidation of benzyl alcohol in aqueous solution. The reactions with Fe_3O_4@PPy-Pt(EG) took place at 40℃ for 8 h in the absence of base to gave a mixture of benzaldehyde and benzoic acid in 81% and 13% yields, respectively (Table 1, entry 1). In contrast, Fe_3O_4@PPy-Pt(NaBH₄) exhibited slightly lower catalytic activity, probably due to their large particle size (entry 2). To further address this issue, alcohol substrates with different electron densities were introduced as probes to examine the catalytic activities of Fe_3O_4@PPy-Pt(EG) and Fe_3O_4@PPy-Pt(NaBH₄), and the results were shown in Table 1 (entry 9-19). When the aerobic oxidation was performed with para-substituted benzyl alcohols, the electron-donating group facilitated the reaction. Compared to benzyl alcohol, 4-mthylbenzyl alcohol, 4-chlorobenzyl alcohol

and 4-methoxybenzyl alcohol showed a higher conversion, while 4-nitrobenzyl alcohol showed a lower conversion over both Fe_3O_4@PPy-Pt(EG) and Fe_3O_4@PPy-Pt(NaBH₄) catalysts. Both catalysts showed higher catalytic activity for substituted aromatic alcohols containing electron-donating group (-CH₃, -OCH₃ and -Cl) than those containing electro-withdrawing group (-NO₂), implying that the electronic effects and intrinsic properties of Pt NPs over these two catalysts were the same[13f]. On the other hand, while the conversions over Fe_3O_4@PPy-Pt(EG) were constantly higher than Fe_3O_4@PPy-Pt(NaBH₄) for different aromatic alcohols, the selectivities toward benzaldehyde over these two catalysts were similar. This illustrated the EG reduced small Pt NPs was only beneficial to improve the conversion of benzylic alcohols aerobic oxidation not the selectivity of benzaldehyde. In addition, both Fe_3O_4@PPy-Pt(EG) and Fe_3O_4@PPy-Pt(NaBH₄) exhibited better catalytic properties than those already reported as shown in Table 1, entry 5-8, 11-13.[13f, 15]

Table 2 Hydrogenation reduction of various nitroaromatics in ethanol

Cat (0.5 mol % of Pt) / Ethanol; H$_2$ (1 atm); R.T. — R–C$_6$H$_4$–NO$_2$ → R–C$_6$H$_4$–NH$_2$

Entry	Substrate	Catalyst	Time (min)	Yield (%)
1		Pt/EG[a]	40	>99
2	(nitrobenzene)	Pt/NaBH$_4$[b]	40	>99
3		Pt/EG	40	92.5[c]
4		Pt/NaBH$_4$	40	95.1[d]
3		Pt/EG	40	98.7
4	Cl–C$_6$H$_4$–NO$_2$	Pt/NaBH$_4$	40	98.2
5		Pt/EG	40	98.4
6	Br–C$_6$H$_4$–NO$_2$	Pt/NaBH$_4$	40	98.0
7		Pt/EG	40	97.7
8	(methyl)	Pt/NaBH$_4$	40	97.5
9		Pt/EG	40	>99
10	HO–C$_6$H$_4$–NO$_2$	Pt/NaBH$_4$	40	>99
11		Pt/EG	40	95.2
12	H$_3$CO–C$_6$H$_4$–NO$_2$	Pt/NaBH$_4$	40	95.6
13		Pt/EG	60	85.5
14		Pt/EG	120	88.6
15	H$_2$N–C$_6$H$_4$–NO$_2$	Pt/NaBH$_4$	60	88.8
16	NO$_2$	Pt/EG	90	90.3
17		Pt/EG	180	92.9
18	(naphthalene)	Pt/NaBH$_4$	90	95.5
19		Pt/EG	240	67.3
20	ClH$_2$C–C$_6$H$_4$–NO$_2$	Pt/EG	480	71.6
21		Pt/NaBH$_4$	240	81.9
22	Cl	Pt/EG	240	18.4
23		Pt/EG	480	20.7
24	(dichloronitrobenzene)	Pt/NaBH$_4$	240	37.2

[a] Fe$_3$O$_4$@PPy-Pt(EG); [b] Fe$_3$O$_4$@PPy-Pt(NaBH$_4$); [c, d] Yield after 5 runs

In order to give a relevant conclusion about sizes effects of the supported Pt NPs catalysts, the catalytic activities were also tested for the hydrogenation of a variety of nitroaromatics to their corresponding products. The reactions were carried out in ethanol at room temperature and under 1 atm pressure of H$_2$. Detailed observations of all the reactions were given in Table 2. In contrast to aerobic oxidation reactions, catalytic properties of Fe$_3$O$_4$@PPy-Pt(EG) and Fe$_3$O$_4$@PPy-Pt(NaBH$_4$) for hydrogenation of most nitroaromatics were almost the same (entry 1, 2, 5-12), being very active for the hydrogenation reaction under such mild conditions and affording over 95% yield of aminobenzene. It was worth noting that Fe$_3$O$_4$@PPy-Pt(NaBH$_4$) gave better activities to several nitroaromatics which were relatively difficult to be hydrotreated under the same conditions (entry 13-24). Interestingly, along with the increase of

the difficulty of the hydrogenation reaction, the gap between the yields got by the two catalysts was widening in the same reaction time. For instance, the yield of 2, 5-dichloroaniline catalyzed by Fe$_3$O$_4$@PPy-Pt(NaBH$_4$) achieved 37.2% (entry 24) — more than twice the yield by Fe$_3$O$_4$@PPy-Pt(EG) (entry 22). And even if the reactions time catalyzed by Fe$_3$O$_4$@PPy-Pt(EG) had been doubled, the yields of phenylamines were still lower than yields catalyzed by Fe$_3$O$_4$@PPy-Pt(NaBH$_4$), indicating these hydrogenation reactions had achieved the final stages of reactions in the corresponding time. This might be due to the better crystal structure of NaBH$_4$ reduced Pt NPs, which probably be in favour of improving catalytic activities.
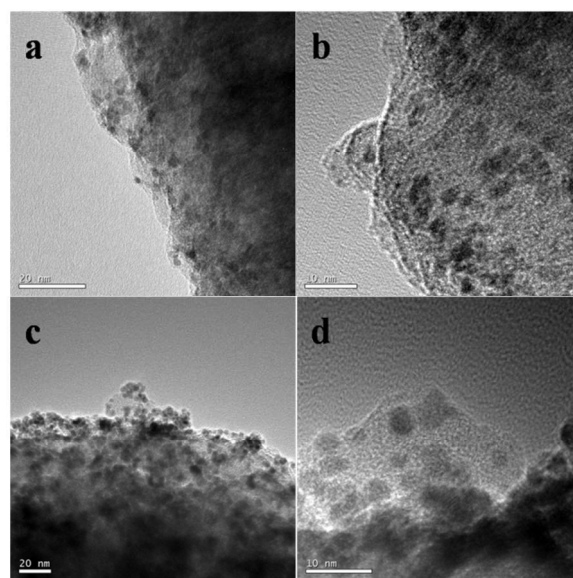

Fig. 7 TEM images of (a) Fe$_3$O$_4$@PPy-Pt(EG) and (c) Fe$_3$O$_4$@PPy-Pt(NaBH$_4$); HRTEM images of (b) Fe$_3$O$_4$@PPy-Pt(EG) and (d) Fe$_3$O$_4$@PPy-Pt(NaBH$_4$) after 5 runs of nitroaromatics hydrogenation

The recycling experiment of the catalyst was further investigated because the recyclability of the heterogeneous catalyst was one of the most important issues for practical applications. Both catalysts could be recycled 5 times for the two reactions, while less than 10% loss of conversion after recycle reactions was observed (Table 1. entry 3, 4 and Table 2. entry 3, 4). Interestingly, after 5 times recycle reactions, Fe$_3$O$_4$@PPy-Pt(NaBH$_4$) showed a lesser loss of activities for both aerobic oxidation of benzylic alcohols and hydrogenation reduction of nitroaromatics than Fe$_3$O$_4$@PPy-Pt(EG). Therefore, the EG reduced Fe$_3$O$_4$@PPy-Pt catalyst exhibited slightly poorer stability than the NaBH$_4$ reduced Fe$_3$O$_4$@PPy-Pt catalyst in the recycle tests, which might due to the agglomeration of small Pt NPs. In order to certify this assumption, TEM and HRTEM were used to observe the morphology of Pt NPs after 5 runs of nitroaromatics hydrogenation, as shown in Fig. 7. Compared with Pt NPs of Fe$_3$O$_4$@PPy-Pt(NaBH$_4$) before the reactions (Fig. 4d, e), it could be concluded that Pt NPs of Fe$_3$O$_4$@PPy-Pt(NaBH$_4$) after 5 runs had no obvious change in running process, except that its crystal structure was unable to be easily observed (Fig. 7c, d). However, Pt NPs of Fe$_3$O$_4$@PPy-Pt(EG) after 5 runs exhibited an apparent agglomeration of Pt NPs (Fig. 7a, b), compared with Pt NPs of Fe$_3$O$_4$@PPy-Pt(EG) before the reactions (Fig. 4a, b).

Conclusion

In conclusion, we used NaBH$_4$ and EG as classical reducing agent to successfully prepare highly dispersed different diameters of Pt nanoparticles supported on PPy-coated Fe$_3$O$_4$. As expected, the chemical reduction methods remarkably affected the size of Pt nanoparticles — about 5.5nm and 2.5nm, respectively. The prepared catalysts exhibited high catalytic activity and good stability for aerobic oxidation of benzylic alcohols and hydrogenation reduction of nitroaromatics. It was highlighted that Fe$_3$O$_4$@PPy-Pt(EG) afforded a higher conversion for benzylic alcohols aerobic oxidation, while the selectivity toward benzaldehyde over these two catalysts was similar. However, catalytic performances for hydrogenation reduction of a majority of nitroaromatics of two catalysts were almost the same. More interesting, Fe$_3$O$_4$@PPy-Pt(NaBH$_4$) gave better activities of several nitroaromatics which were relatively difficult to be hydrotreated under the same conditions. Furthermore, both catalysts could be recycled 5 times for the two reactions, while less than 10% loss of conversion after recycle reactions is observed. And because of the agglomeration of small Pt nanoparticles, the EG reduced Fe$_3$O$_4$@PPy-Pt catalyst exhibited slightly poorer stability than the NaBH$_4$ reduced Fe$_3$O$_4$@PPy-Pt catalyst in the recycle tests. Our work demonstrated the important role of reducing agents for immobilizing Pt nanoparticles. It also could be obtained that size effects might be quietly different for different kinds of reactions. Sometimes, superior crystal structure was probably more meaningful than smaller size diameter for a certain kind of reaction. It is surely that preparing smaller metal nanoparticles with prefect crystal structure and avoiding interaction agglomeration can greatly improve catalytic activities.

Acknowledgements

References

1 (a) A. T. Bell, *Science*, 2003, **299**, 1688; (b) R. A. van Santen, *Acc. Chem. Res.*, 2009, **42**, 57; (c) G. A. Somorjai and J. Y. Park, *Angew. Chem. Int. Ed.*, 2008, **47**, 9212; (d) G. A. Somorjai, H. Frei and J. Y. Park, *J. Am. Chem. Soc.*, 2009, **131**, 16589.

2 (a) S. F. Chen, J. P. Li, K. Qian, W. P. Xu, Y. Lu, W. X. Huang and S. H. Yu, *Nano Res.*, 2010, **3**, 244; (b) L. De Rogatis, M. Cargnello, V. Gombac, B. Lorenzut, T. Montini, P. Fornasiero, *ChemSusChem*, 2010, **3**, 24; (c) M. Nasrollahzadeh, *New J. Chem.*, 2014, **38**, 5544; (d) L. Tian, T. M. Cronin and Y. Weizmann, *Chem. Sci.*, 2014, **5**, 4153; (e) G. A. Somorjai and J. Y. Park, *Chem. Soc. Rev.*, 2008, **37**, 2155.

3 G. Liu, M. J. Arellano-Jiménez, C. B. Carter and A. G. Agrios, *J. Nanopart. Res.*, 2013, **15**, 1744.

4 (a) Y. Bing, H. Liu, L. Zhang, D. Ghosh and J. Zhang, *Chem. Soc. Rev.*, 2010, **39**, 2184; (b) S. Pande, M. G. Weir, B. A. Zaccheo and R. M. Crooks, *New J. Chem.*, 2011, **35**, 2054; (c) M. Giovanni, H. L. Poh, A. Ambrosi, G. Zhao, Z. Sofer, F. Šaněk, B. Khezri, R. D. Webster and M. Pumera, *Nanoscale*, 2012, **4**, 5002; (d) Y. Nie, S. Chen, W. Ding, X. Xie, Y. Zhang and Z. Wei, *Chem. Commun.*, 2014, DOI: 10.1039/C4CC06781A.

5 (a) O. Tomita, B. Ohtani and R. Abe, *Catal. Sci. Technol.*, 2014, **4**, 3850; (b) R. Li, W. Chen, H. Kobayashi and C. Ma, *Green Chem.*, 2010, **12**, 212; (c) D. Marquardt, F. Beckert, F. Pennetreau, F. Töle,

R. Mülhaupt, O. Riant, S. Hermans, J. Barthel and C. Janiak, *Carbon*, 2014, **66**, 285.

6 (a) R. S. Dey and C. R. Raj, *J. Phys. Chem. C.*, 2010, **114**, 21427; (b) Z. Wen, S. Ci and J. Li, *J. Phys. Chem. C.*, 2009, **113**, 13482.

7 (a) M. Bouallega, S. Norsic, D. Baudouin, R. Sayah, E. A. Quadrelli, J-M. Basset, J-P. Candy, P. Delichere, K. Pelzer, L. Veyre and C. Thieuleux, *J. Catal.*, 2011, **284**, 184; (b) M. Xie, F. Zhang, Y. Long and J. Ma, *RSC Adv.*, 2013, **3**, 10329; (c) M. Chatterjee, Y. Ikushima and F. Zhao, *New J. Chem.*, 2003, **27**, 510; (d) H. Bönnemann, W. Wittholt, J. D. Jentsch and A. S. Tilling, *New J. Chem.*, 1998, **22**, 713; (e) Y. Liu, J. Chung, Y. Jang, S. Mao, B. M. Kim, Y. Wang and X. Guo, *ACS Appl. Mater. Interfaces*, 2014, **6**, 1887; (f) N. Musselwhite and G. A. Somorjai, *Top. Catal.*, 2013, **56**, 1277; (g) J. H. B. Sattler, A. M. Beale and B. M. Weckhuysen, *Phys. Chem. Chem. Phys.*, 2013, **15**, 12095; (h) J. Zhu, T. Wang, X. Xu, P. Xiao and J. Li, *Appl. Catal. B: Environ.*, 2013, **130-131**, 197.

8 Q. Zhang, W. Deng and Y. Wang, *Chem. Commun.*, 2011, **47**, 9275.

9 (a) J. M. Clemente-Juan, E. Coronado and A. Gaita-Ariñ, *Chem. Soc. Rev.*, 2012, **41**, 7464; (b) M. Clemente-León, E. Coronado, C. Martí-Gastaldoz and F. M. Romero, *Chem. Soc. Rev.*, 2011, **40**, 473; (c) E. Coronado and G. M. Espallargas, *Chem. Soc. Rev.*, 2013, **42**, 1525; (d) J. P. Malrieu, R. Caballol, C. J. Calzado, C. Graaf and N. Guihéry, *Chem. Rev.*, 2014, **114**, 429; (e) J. Thévenot, H. Oliveira, O. Sandre and S. Lecommandoux, *Chem. Soc. Rev.*, 2013, **42**, 7099; (f) X-Y. Wang, C. Avendaño and K. R. Dunbar, *Chem. Soc. Rev.*, 2011, **40**, 3213; (g) J. Yuan, Y. Xu and A. H. E. Müller, *Chem. Soc. Rev.*, 2011, **40**, 640.

10 (a) M. A. M. Gijs, F. Lacharme and U. Lehmann, *Chem. Rev.*, 2010, **110**, 1518; (b) J. H. Jung, J. H. Lee and S. Shinkai, *Chem. Soc. Rev.*, 2011, **40**, 4464; (c) S. Laurent, D. Forge, M. Port, A. Roch, C. Robic, L. V. Elst and R. N. Muller, *Chem. Rev.*, 2008, **108**, 2064; (d) A-H. Lu, E. L. Salabas and F. Schüth, *Angew. Chem. Int. Ed.*, 2007, **46**, 1222; (e) Y. Pan, X. Du, F. Zhao and B. Xu, *Chem. Soc. Rev.*, 2012, **41**, 2912; (f) L. H. Reddy, J. Arias, J. Nicolas and P. Couvreur, *Chem. Rev.*, 2012, **112**, 5818.

11 (a) R. Abu-Reziq, D. Wang, M. Post and H. Alper, *Chem. Mater.*, 2008, **20**, 2544; (b) Y. Q. Wang, B. F. Zou, T. Gao, X. P. Wu, S. Y. Lou and S. M. Zhou, *J. Mater. Chem.*, 2012, **22**, 9034; (c) L. Gai, X. Han, Y. Hou, J. Chen, H. Jiang and X. Chen, *Dalton Trans.*, 2013, **42**, 1820; (d) V. Polshettiwar, R. Luque, A. Fihri, H. Zhu, M. Bouhrara and J. M. Basset, *Chem. Rev.*, 2011, **111**, 3036.

12 (a) Y. Long, M. Xie, J. Niu, P. Wang and J. Ma, *Appl. Surf. Sci.*, 2013, **277**, 288; (b) J. Niu, M. Liu, P. Wang, Y. Long, M. Xie, R. Li and J. Ma, *New J. Chem.*, 2014, **38**, 1471; (c) J. Niu, M. Xie, X. Zhu, Y. Long, P. Wang, R. Li and J. Ma, *J. Mol. Catal. A: Chem.*, 2014, **392**, 247; (d) P. Wang, F. Zhang, Y. Long, M. Xie, R. Li and J. Ma, *Catal. Sci. Technol.*, 2013, **3**, 1618; (e) P. Wang, H. Liu, M. Liu, R. Li and J. Ma, *New J. Chem.*, 2014, **38**, 1138; (f) X. Zhu, J. Niu, F. Zhang, J. Zhou, X. Li and J. Ma, *New J. Chem.*, 2014, **38**, 4622.

13 (a) J. Kugai, S. Seino, T. Nakagawa and T. A. Yamamoto, *J. Nanopart. Res.*, 2014, **16**, 2275; (b) N. Hickey, P. Fornasiero, J. Kašpar, M. Graziani, G. Blanco and S. Bernal, *Chem. Commun.*, 2000, 357; (c) C. K. Rhee, B-J. Kim, C. Ham, Y-J. Kim, K. Song and K. Kwon, *Langmuir*, 2009, **25**, 7140; (d) T. Wang, H. Shou, Y. Kou and H. Liu, *Green Chem.*, 2009, **11**, 562; (e) J. Xing, Y. H. Li, H. B. Jiang, Y. Wang and H. G. Yang, *Int. J. Hydrogen Energ.*, 2014, **39**, 1237; (f) C. Zhou, H. Chen, Y. Yan, X. Jia, C-J. Liu and Y. Yang, *Catal. Today*, 2013, **211**, 104.

14 K. Cheah, M. Forsyth and V. T. Truong, *Synth. Met.*, 1998, **94**, 215.

15 (a) Y. H. Ng, S. Ikeda, T. Harada, Y. Morita and M. Matsumura, *Chem. Commun.*, 2008, 3181. (b) A. Ohtaka, Y. Kono, S. Inui, S. Yamamoto, T. Ushiyama, O. Shimomura and R. Nomura, *J. Mol. Catal. A: Chem.*, 2012, **360**, 48.